

Temperature Dependence of Local Motions in Glassy Polycarbonate from Carbon and Proton Nuclear Magnetic Resonance

J. F. O'Gara, A. A. Jones,* and C.-C. Hung

Jeppson Laboratory, Department of Chemistry, Clark University,
Worcester, Massachusetts 01610

P. T. Inglefield

Department of Chemistry, College of the Holy Cross, Worcester, Massachusetts 01610.
Received September 21, 1984

ABSTRACT: Carbon-13 chemical shift anisotropy (CSA) line shapes and proton relaxation data are used to establish the time scale and amplitudes of phenylene group motions in glassy polycarbonate as a function of temperature. The phenylene group undergoes both π flips and restricted rotation. The rate of π flips and the amplitude of restricted rotation are determined from simulating the carbon-13 CSA line shapes. When a simple exponential correlation function is used, an activation energy of 11 ± 5 kJ/mol is found for the π flip rate. The root mean square angular amplitude varies linearly with temperature to the one-half power. The π flip rate is found to lie on the same line on a relaxation map as the proton relaxation minima, dielectric loss maxima, and dynamic mechanical loss maxima. Analysis of the relaxation map gives an apparent activation energy of 48 ± 5 kJ/mol. The discrepancy between the two activation energies arises from the limited frequency range and simple correlation function employed in the CSA analysis. A Williams-Watts-Ngai fractional exponential correlation function with Arrhenius parameters set from the relaxation map can account for the breadth and position of the proton relaxation minima and the dynamic mechanical loss peak.

Introduction

Over the past few decades there has been considerable interest in using NMR to define and quantify the motional processes which occur in bulk polymers below the glass transition temperature, T_g .^{1,2} At temperatures greater than T_g , a polymer chain may undertake a wide variety of motions; however, below T_g many of these become modified, in particular the long-range motions. Polymers frequently reveal secondary transitions which are thought to arise from specific types of local motion still present in the glass.

One group of polymers in particular, the polycarbonate of bisphenol A (BPA) and its structurally related analogues, has received much attention. This intense interest is fueled by the fact that BPA exhibits good impact resistance over a temperature range more than 250 °C below the glass transition temperature ($T_g \sim 145$ °C).³ Dynamic mechanical and dielectric spectroscopy studies at 1 Hz reveal that BPA has an especially prominent secondary transition peak at approximately -100 °C.⁴⁻⁷ It can be noted that nearly all glassy polymers which exhibit high-impact strength have prominent secondary transitions, thus arguing for some relationship between the bulk mechanical properties and the extensive, rapid motion in the glass.⁸

Recently there has been significant structural and dynamical information developed on the polycarbonates from NMR.⁹⁻¹² In particular, the geometry of the phenylene group reorientation in BPA in the limit of rapid motion in the bulk below T_g has been characterized through the use of deuterium,¹³ chemical shift anisotropy (CSA),¹² and dipolar rotational spin-echo carbon-13 line shapes.¹⁵ The basic conclusion reached by all is that the principal motion of the phenylene groups may be characterized as π flips about the C_1C_4 axis in combination with a small restricted angular oscillation of approximately 30-40° about the same axis. In this report, the previous CSA line shape analysis for a sample of carbon-13-labeled BPA, where 90% of one of the two phenylene carbons ortho to the carbonate are isotopically enriched, is extended over the temperature range of -160 to +120 °C in an attempt to characterize the rate and amplitude of the phenylene group motion as a function of temperature.

On its own, such a study suffers from the limited frequency dependence of the changing chemical shift anisotropy dispersion. To circumvent this problem, proton spin-lattice relaxation times, T_1 's, at the Larmor frequency of 90 MHz and spin-lattice relaxation times in the rotating frame, $T_{1\rho}$'s, are measured for a methyl-deuterated analogue of BPA (BPA- d_6) so that a more thorough analysis of the time scales and energetics of the phenylene motion may be obtained. These latter studies parallel an earlier proton analysis of the chloral polycarbonate¹¹ in which a quantitative interpretation of the phenylene proton relaxation data was offered based on a homogeneous correlation function¹⁶ for motional modulation of the dipole-dipole interaction. The greatest interpretational success was obtained by using a fractional exponential correlation function which has been developed on the basis of correlated state excitation in condensed matter by Ngai¹⁷⁻¹⁹ and empirically by Williams and Watts.²⁰ As with the chloral polycarbonate, if the NMR relaxation data for BPA- d_6 can be successfully quantified with the correlation function, then the temperature-dependent spectral densities obtained from the spin relaxation studies can be used to predict the temperature and frequency of the dynamic mechanical response.

Experimental Section

The polycarbonate of bisphenol A, single-site carbon-13 enriched (>90%) on one of the two phenylene carbons ortho to the carbonate, was synthesized from enriched phenol (2-carbon-13) obtained from KOR Isotopes, Inc. The methyl-deuterated analogue of the bisphenol A polycarbonate was obtained from standard synthetic techniques.²¹ The methyl groups were found to be 97% deuterated as determined from proton and deuterium spectra of the dissolved polymer.

The carbon CSA spectra were obtained for a dried powdered sample by using cross polarization followed by high-power proton decoupling at a carbon frequency of 22.636 MHz and a proton frequency of 89.995 MHz. Rotating fields of about 1.0 mT for protons and 4.0 mT for carbon were used with a contact time of 3 ms. Several hundred free induction decays were averaged at each temperature before Fourier transformation to give the absorption spectra. Line shapes recorded without cross polarization were found to be experimentally indistinguishable. To obtain a standard reference for the line shapes at each temperature, the first moment was numerically calculated for each spectrum and

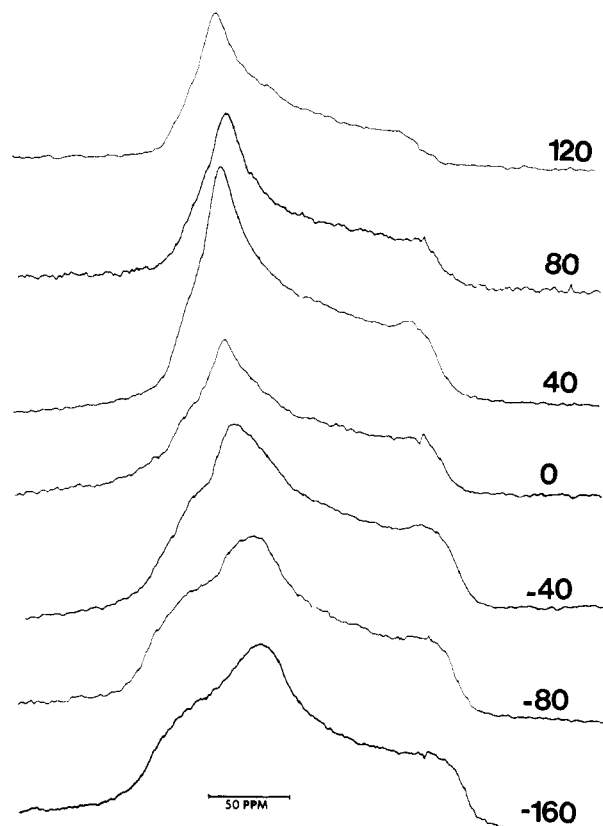


Figure 1. Carbon-13 CSA line shapes at several temperatures.

assigned the value of 72.5 ppm on the CS_2 scale, which is the isotopic shift found for this phenylene carbon in solution.

Proton spin-lattice relaxation times for a dried powdered sample of BPA- d_6 were measured at the Larmor frequency of 90 MHz. The $\pi/2$ pulse width was 2 μs ; and a standard $\pi-\tau-\pi/2$ pulse sequence was used with a cycle time greater than 5 times T_1 . Proton spin-lattice relaxation times in the rotating frame were measured at a radio frequency field strength of 1.0 mT by using a standard $\pi/2$ -phase shifted locking pulse sequence.

All NMR measurements were made with a Bruker SXP 20-100 spectrometer. Temperature control was maintained to within ± 2 K with a Bruker B-ST 100/700 temperature controller.

Results

The temperature dependence of the changing CSA line shape is shown in Figure 1.

For the proton spin-lattice relaxation data at 90 MHz, the decay of the magnetization at all temperatures follows a simple exponential dependence with delay time, τ . The spin-lattice relaxation time, T_1 , is easily calculated from a linear least-squares analysis of $\ln(A_\infty - A_\tau)$ vs. τ , where the A 's are signal amplitudes and τ is the delay time. The uncertainty in a given T_1 value is $\pm 10\%$.

The proton $T_{1\rho}$ data are characterized from a linear least-squares analysis of $\ln A$ vs. τ , where A is still the signal amplitude but τ is now the length of the locking pulse. The deviations from simple exponential decay are small and not indicative of a dispersion of relaxation times so a fit of the whole curve to a single exponential decay is employed. Similar behavior was previously reported for the proton $T_{1\rho}$ decay curves of the chloral polycarbonate. The error in a given $T_{1\rho}$ value is $\pm 15\%$ and both T_1 and $T_{1\rho}$ data are summarized as a function of temperature in Figure 2.

Interpretation

CSA Tensor Line Shapes. The carbon-13-labeled polycarbonate allows one to study the chemical shift anisotropy line shape of this phenylene carbon. The principal

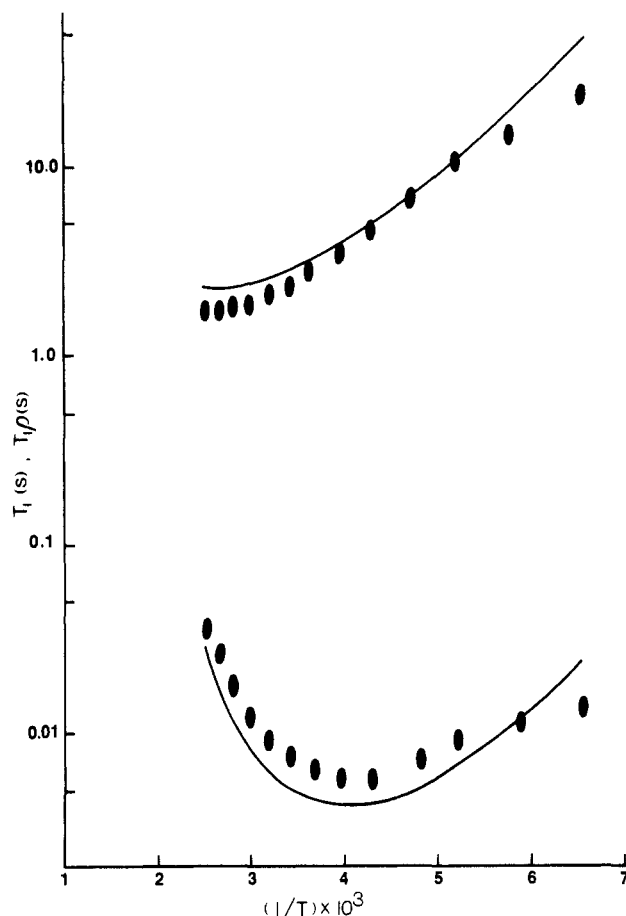


Figure 2. Proton spin-lattice relaxation times and proton spin-lattice relaxation times in the rotating frame vs. inverse temperature. The solid line corresponds to a fit of the relaxation data with a Williams-Watts-Ngai fractional exponential correlation function.

axis system for the chemical shift tensor of aromatic carbons, as reported for benzene,²² is oriented with the σ_{11} axis parallel to the C-H bond and the σ_{33} axis perpendicular to the ring plane. The σ_{22} axis is in the ring plane, perpendicular to the C-H bond. In the previous communication,¹⁴ the principal values of the shielding tensor were calculated by matching theoretical spectra generated on the basis of the Bloembergen-Rowland equations²³ with the experimental spectra at -160°C . A reasonably good fit between calculated and observed spectra is found by using $\sigma_{11} = 17 \pm 1$, $\sigma_{22} = 52 \pm 1$, and $\sigma_{33} = 175 \pm 1$ ppm on the CS_2 scale and a Lorentzian line broadening of 320 Hz. In simulating σ_{11} , σ_{22} , and σ_{33} , we assume that the frequency of all molecular reorientations is small compared to $\sigma_{11} - \sigma_{33}$ at -160°C . This is a good assumption as even at -140 and -120°C the spectra can be simulated with these values; and thus we have met the "rigid-lattice" condition. These principal values correspond to an isotropic chemical shift of 70 ± 3 ppm, which compares well with the observed chemical shift in solution of 72.5 ppm.

With the onset of motion, the chemical shift tensor will be averaged depending on the character of the geometry and rate of reorientation. If the nucleus under examination was undergoing fast, random reorientation, then the chemical shift tensor would be reduced to just its isotropic value, as is evident for a rapidly tumbling molecule in solution. For a restricted reorientation or a slowly reorienting molecule, only a part of the chemical shift dispersion will be averaged out and the spectrum will change accordingly. Having defined the principal values of the shielding tensor and possessing knowledge of their orien-

tation in the molecular frame, we modeled possible motions for the phenylene group in an attempt to simulate the highest temperature spectra at +120 °C. The line shape at this temperature is narrower and closer to an axially symmetric line shape when compared to the -160 °C spectrum. At this temperature we can assume that the molecular reorientation occurs at a rapid rate, where rapid means the correlation time is much shorter than the inverse of the spectral width involved. Thus, we can calculate line shapes very simply by replacing the rigid shielding tensor with a tensor averaged over the geometry of the motion through the use of Euler transformation matrices and the appropriate angular weighting functions as outlined by Slotfeldt-Ellingsen and Resing²⁴ and Wemmer et al.^{25,26}

In this calculation one begins with the shielding tensor, σ_{123} , in the principal axis system

$$\sigma_{123} = \begin{vmatrix} \sigma_{11} & 0 & 0 \\ 0 & \sigma_{22} & 0 \\ 0 & 0 & \sigma_{33} \end{vmatrix} \quad (1)$$

To consider the effects of molecular motion the shielding tensor is transformed to the axis system of molecular motion by use of an Euler transformation matrix \mathbf{R} . The orientation of the new frame with respect to a previous one is defined by a set of Euler angles, $\Omega = \alpha, \beta, \gamma$. If a positive rotation is to be applied to a frame (x, y, z) about the Euler angles (α, β, γ), then

$$\mathbf{R}(\alpha\beta\gamma) = \mathbf{R}_z(\gamma)\mathbf{R}_y(\beta)\mathbf{R}_x(\alpha) \quad (2)$$

where α is a rotation about the original z axis, β is about the new y axis, and γ is about the final z axis. The product of the three rotation matrices leads to

$$\mathbf{R}(\alpha\beta\gamma) = \begin{vmatrix} \cos \alpha \cos \beta \cos \gamma - \sin \alpha \cos \beta \cos \gamma + & -\sin \beta \cos \gamma \\ \sin \alpha \sin \gamma & \cos \alpha \sin \gamma \\ -\cos \alpha \cos \beta \sin \gamma - \sin \alpha \cos \beta \sin \gamma + & \sin \beta \sin \gamma \\ \sin \alpha \cos \gamma & \cos \alpha \cos \gamma \\ \cos \alpha \sin \beta & \sin \alpha \sin \beta & \cos \beta \end{vmatrix} \quad (3)$$

An appropriate orientation of the molecular motion axis frame places the x axis parallel to the C_1C_4 axis of the phenylene group so

$$\mathbf{R}(\delta) = \begin{vmatrix} \cos \delta & -\sin \delta & 0 \\ \sin \delta & \cos \delta & 0 \\ 0 & 0 & 1 \end{vmatrix} \quad (4)$$

with $\delta = 60^\circ$ for the labeled carbon of interest. The shielding tensor in the molecular motion axis system σ_{xyz} is then given by

$$\sigma_{xyz} = \mathbf{R}(\delta) \cdot \sigma_{123} \cdot \mathbf{R}(\delta)^{-1} \quad (5)$$

One can now model the effect on the shielding of different motions of the phenylene group about the C_1C_4 axis. For instance, rotating the molecule about the x axis by angle α' is defined by

$$\sigma_{xyz}(\alpha') = \mathbf{R}(\alpha') \cdot \sigma_{xyz} \cdot \mathbf{R}(\alpha')^{-1} \quad (6)$$

where

$$\mathbf{R}(\alpha') = \begin{vmatrix} 1 & 0 & 0 \\ 0 & \cos \alpha' & -\sin \alpha' \\ 0 & \sin \alpha' & \cos \alpha' \end{vmatrix}$$

For rapid flipping of the phenylene group between two angular positions, separated by an angle α' , the motionally averaged shielding tensor, σ_{flip} , is given by

$$\sigma_{\text{flip}} = (1/2)(\sigma_{xyz} + \sigma_{xyz}(\alpha')) \quad (7)$$

Another possible type of molecular reorientation that we may consider is rapid phenylene group rotation about the x axis through all angular positions or through a limited angular range. We can model this type of motion by averaging over σ in eq 6.

$$\langle \sigma_{xyz} \rangle_{\alpha'} = \langle \mathbf{R}(\alpha') \cdot \sigma_{xyz} \cdot \mathbf{R}(\alpha')^{-1} \rangle_{\alpha'} \quad (8)$$

The method of averaging depends on the potential function chosen to describe how the molecule is allowed to spend time between the end points of its oscillations. For example, if one assumes a square well potential, then one may calculate each tensor element of $\langle \sigma_{xyz} \rangle$ as follows:

$$\langle \sigma_{xyz}(i,j) \rangle_{\alpha'} = \int_{-\alpha'/2}^{+\alpha'/2} \mathbf{R}(\alpha') \cdot \sigma_{xyz}(i,j) \mathbf{R}(\alpha')^{-1} d\alpha' / \int_{-\alpha'/2}^{+\alpha'/2} d\alpha' \quad (9)$$

The resultant matrix $\langle \sigma_{xyz} \rangle_{\alpha'}$ may then be diagonalized to obtain three new average values, σ_{11} , σ_{22} , and σ_{33} , which correspond to the averaged tensor. The characteristic line shape may then be calculated with the equation²³

$$I(\sigma; \sigma_{11}, \sigma_{22}, \sigma_{33}, \Delta\sigma) = \int_{-\infty}^{+\infty} I^0(\sigma - \xi; \sigma_{11}, \sigma_{22}, \sigma_{33}) f(\xi; \Delta\sigma) d\xi \quad (10)$$

For $\sigma_{33} \leq \sigma < \sigma_{22}$

$$I^0(\sigma; \sigma_{11}, \sigma_{22}, \sigma_{33}) = \pi^{-1} K(x) (\sigma_{11} - \sigma)^{-0.5} (\sigma_{22} - \sigma_{33})^{-0.5} \\ x = (\sigma_{11} - \sigma_{22})(\sigma - \sigma_{33}) / [(\sigma_{22} - \sigma_{33})(\sigma_{11} - \sigma)]$$

For $\sigma_{22} < \sigma \leq \sigma_{11}$

$$I^0(\sigma; \sigma_{11}, \sigma_{22}, \sigma_{33}) = \pi^{-1} K(x) (\sigma - \sigma_{33})^{-0.5} (\sigma_{11} - \sigma_{22})^{-0.5} \\ x = (\sigma_{11} - \sigma)(\sigma_{22} - \sigma_{33}) / [(\sigma - \sigma_{33})(\sigma_{11} - \sigma_{22})]$$

For $\sigma < \sigma_{11}$, and $\sigma > \sigma_{33}$

$$I^0(\sigma; \sigma_{11}, \sigma_{22}, \sigma_{33}) = 0$$

And

$$K(x) = \int_0^{\pi/2} (1 - X^2 \sin^2 \Psi)^{-1} d\Psi$$

$$f = (\xi, \Delta\sigma) = 1 / (1 + (2\xi/\Delta\sigma)^2)$$

where f describes the Lorentzian line broadening of the chemical shift dispersion, and I^0 and the carbon chemical shifts increase toward lower fields. In the earlier communication, we reported on comparisons of various line shapes generated on this basis with the high-temperature line shape. It was found that the most probable motional model suggested that the phenylene motion takes place about the C_1C_4 axis in the form of jumps between two minima separated by 180° (π flips) in combination with a restricted rotation over $\pm 30^\circ$ around each minimum. It should be noted here that there was a small ppm referencing problem in the earlier CSA study that was corrected here when interpreting the temperature dependence of the other CSA line shapes. The basic conclusions are the same although in the final modeling the restricted rotation occurs over a greater range, $\pm 36^\circ$, than previously reported for +120 °C. The oscillation is modeled as a restricted diffusion over an angular range using the square well potential.

Employing the interpretation of the geometry of the phenylene motion at +120 °C as a starting point, one can simulate the temperature dependence of the changing CSA line shapes. From +120 to +20 °C, the π flips are in the limit of rapid motion as the line shapes can be described by a tensor and thus this molecular motion can still be

modeled rather easily through the use of Euler transformation matrices and the appropriate angular weighting functions. In this temperature region, the line shapes are all of the same general shape as observed at +120 °C, although the σ_{11} and σ_{33} components of the averaged tensor move to make the spectra slightly broader as temperature decreases. One can simulate this line shape behavior, first, by assuming the π flips are occurring at a rapid rate and, second, by simply decreasing the amplitude of the restricted rotation with temperature.

If the molecular motion occurs at a frequency comparable to the spectral width, the line shape may no longer be described by the above approach. For the spectra from 0 to -100 °C, one can no longer assume that the π flips are occurring at a rapid rate and thus one must use a model which allows for an arbitrary rate. We make use of the exchange model for a CSA line shape as described by Mehring²² and Wemmer.²⁵

The line shape equation for a multisite exchange where each site can exchange with any other site is given by

$$g(\omega) = (1/N)(L/(1 - KL)) \quad (11)$$

where

$$L = \sum_{j=1}^N [i(\omega - \omega_j) - (1/T_{2j}) + NK]^{-1}$$

T_{2j} = spin-spin relaxation time

$K = \tau^{-1}$ = exchange or flipping rate

N = number of sites

ω_j = frequency of site j

$$\begin{aligned} \omega_j = & \sigma_{\text{iso}} + (\sigma_{33} - \sigma_{\text{iso}})[P_2(\cos \beta)P_2(\cos \theta) + \\ & (3/4) \sin 2\theta \sin 2\beta \cos 2(\phi + \gamma) - 3 \sin \theta \cos \theta \sin \beta \\ & \cos \beta \cos(\phi + \gamma)] + ((\sigma_{11} - \sigma_{22})/2)[\sin 2\theta \cos 4\beta \cos \\ & (2\phi + \gamma + \alpha) + \sin 2\theta \sin 4\beta \cos(2\phi + \gamma - \alpha)) + \\ & \sin \theta \cos \theta \sin \beta \{(\cos \beta + 1) \cos(\phi + \gamma + 2\alpha) + (\cos \beta \\ & - 1) \cos(\phi + \gamma + 2\alpha)\} + P_2(\cos \theta) \sin^2 \beta \cos(2\alpha)] \end{aligned}$$

and P_2 is the Legendre polynomial. The Euler angles of the flipping axis with respect to the principal axis system of the tensor are (α, β, γ) and the Euler angles of the magnetic field with respect to the molecular frame containing the flipping axis as the z axis are (θ, ϕ) .

In NMR, the real part of $g(\omega)$ is termed the line shape $I(\omega)$.

$$I(\omega) = \text{Re } g(\omega) \quad (12)$$

This equation has been developed for a particular orientation of the molecular frame with respect to the magnetic field. For an isotropic powder sample, one has to average over all orientations

$$I(\Omega) = \int d\Omega P(\Omega)I(\omega, \Omega) \quad (13)$$

where $P(\Omega) = (1/4\pi)$ and $d\Omega = \sin \theta d\theta d\phi$. (A computer program which generates CSA line shapes on the basis of this model can be found in the Ph.D. thesis of Wemmer.²⁵)

In this approach, only a single correlation time is used to describe the flipping process. Starting with the 0 °C line shape, we must decrease the rate of the π flip process with decreasing temperature as the line shape is changing in this region from being axially symmetric in shape to asymmetric. For most of this temperature region, the amplitude of the restricted rotation does not significantly alter the line shape and thus only the rate of the π flips controls the resultant line shape. However, the amplitude

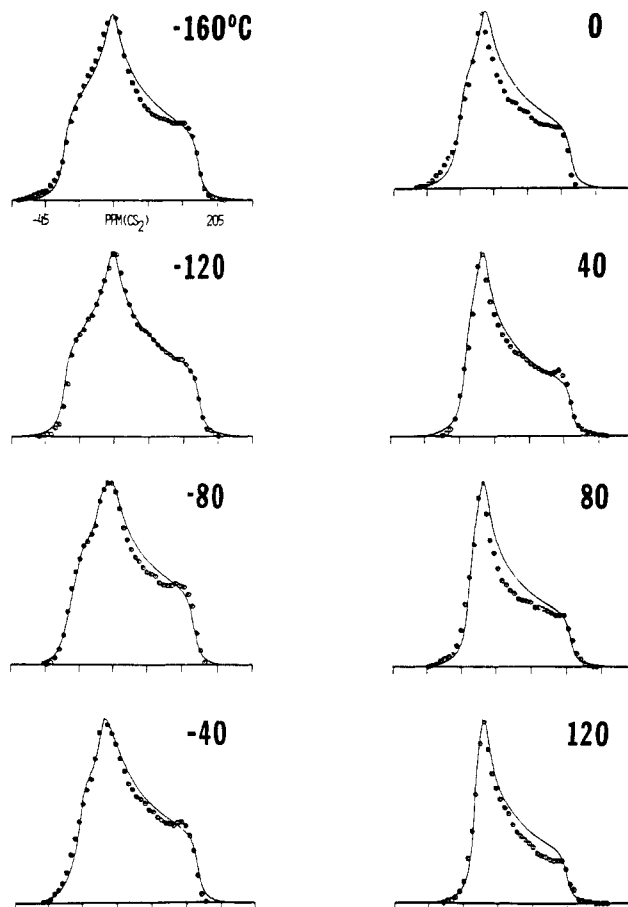


Figure 3. The lines are simulations of the carbon-13 CSA line shapes at several temperatures while the points are line shape data taken from Figure 1.

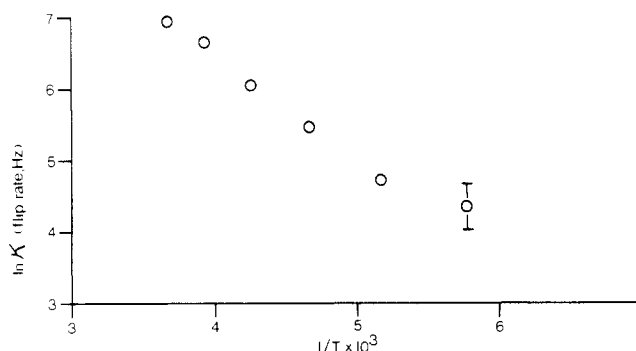


Figure 4. Logarithm of the flip rate vs. inverse temperature. The flip rate is determined from simulation of the carbon-13 CSA line shape.

of the restricted rotation is estimated by extrapolation from the high-temperature region. The π flip rate as a function of temperature is determined by comparing the theoretical and experimental spectra. A summary of line shape comparisons is contained in Figure 3 and the simulations are good with the possible exception of 0 °C. At this temperature both the π flips and the restricted oscillation make comparable contributions to the line narrowing. When two motional processes induce roughly equivalent narrowing, difficulties in line shape simulation are encountered since neither can be assumed to be fast or dominant with respect to the other.²⁵

The results of these simulations are summarized as follows. An Arrhenius analysis of the single correlation times yields an apparent activation energy of 11 ± 5 kJ/mol for the flip process, as shown in Figure 4. This

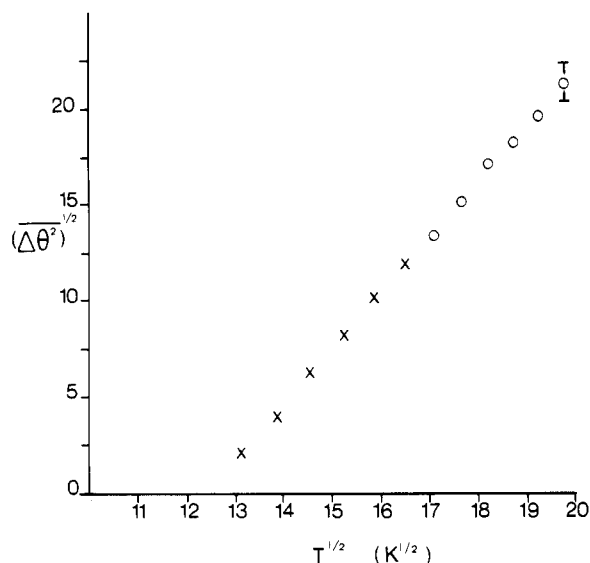


Figure 5. Root mean square amplitude of restricted phenylene group rotation about the C_1C_4 axis vs. temperature to the one-half power. The rms amplitude is determined from simulating the carbon-13 CSA line shapes. The open circles are determined at temperatures where the oscillation is the primary source of narrowing and x's are estimates made at temperatures where the flips are the primary source of narrowing.

number should be treated with caution as it is determined from a sampling of only a few data points over a very small frequency range. Figure 5 is a plot of the root mean square displacement vs. the square root of temperature which provides a summarization of the temperature dependence of the oscillation.

Relaxation Data. The limited frequency range of the changing CSA dispersion does not warrant a more complex interpretation of the time dependence of the phenylene group motion by itself. As mentioned in the Introduction, proton spin-lattice relaxation measurements carried out in both the Zeeman frame and the rotating frame will be used to characterize the rate dependence of the phenylene motion in a similar manner as was done for the chloral polycarbonate.¹¹ Both T_1 and $T_{1\rho}$ can be quantitatively simulated as a function of temperature with a given correlation function and the associated spectra density. The standard T_1 and $T_{1\rho}$ expressions are used¹¹

$$1/T_1 = (2/3)\gamma^2 S [J_1(\omega_H) + 4J_2(2\omega_H)]$$

$$1/T_{1\rho} = (2/3)\gamma^2 S [1.5J_e(2\omega_e) + 2.5J_1(\omega_H) + J_2(2\omega_H)] \quad (14)$$

where $\omega_e = \gamma_H H_{rf}$ and S is the motionally modulated component of the second moment. The applicability of these equations and this approach has been presented for chloral polycarbonate and the current situation is quite similar.

Given the previous success of the fractional exponential correlation function in modeling the relaxation behavior of the chloral polycarbonate, it is again chosen to simulate the BPA- d_6 data. The correlation function can be expressed in the Ngai formalism¹⁷⁻¹⁹ as

$$\phi(t) = \phi(0) \exp[-(t/\tau_p)^{1-n}] \quad (15)$$

where $0 < n < 1$ and

$$\tau_p = [(1-n) \exp(n\gamma) E_c^n \tau_0]^{1/(1-n)} \quad (16)$$

where $\tau_0 = \tau_\infty \exp(E_A/RT)$, the microscopic correlation time, E_c the bath cutoff energy, and $\gamma = 1.577$ Euler's constant. The parameters τ_∞ and E_A fix the microscopic

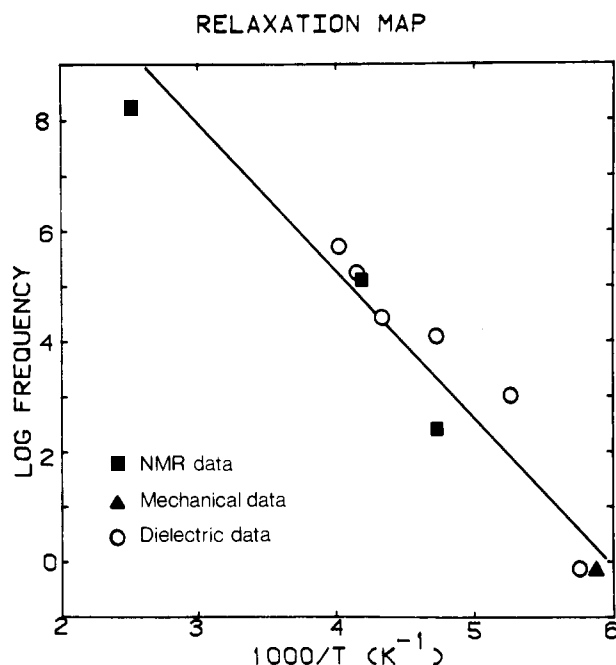


Figure 6. log frequency vs. inverse temperature or relaxation map. The highest frequency NMR point is the 90-MHz proton T_1 minimum. The next highest frequency NMR point is the 43-kHz T_1 minimum. The lowest frequency NMR point is the position of maximum collapse of the carbon-13 chemical shift anisotropy line shape. The open circles are maxima of dielectric loss curves taken at different frequencies. The positions of all points have an uncertainty of the order of 10 degrees because of the breadth of the loss peaks and relaxation minima.

dynamics and energetics of the fundamental process in the absence of correlated state coupling. The parameters n and E_c determine the width of the frequency dispersion and the renormalized time scale due to medium effects. For $n \neq 0$, $\tau_p = \tau_\infty \exp(E_A^*/RT)$ where E_A^* is the apparent activation energy, given by $E_A^* = E_A/(1-n)$ and the apparent preexponential is given by

$$\tau_\infty^* = [(1-n) \exp(n\gamma) E_c^n \tau_0]^{1/(1-n)}$$

The actual parameters varied to fit experimental data are E_A^* , τ_∞^* , and n . In order to get a handle on the values of E_A^* and τ_∞^* for the BPA- d_6 relaxation data, a relaxation map, $\log \nu_c$ vs. T^{-1} , was constructed. The temperature positions of T_1 and $T_{1\rho}$ minima each can be assigned an appropriate correlation frequency as outlined by McCall.¹ One can also associate a correlation frequency with the CSA line shape collapse. The average frequency difference between the two sites corresponding to the two positions of the phenylene group is $\delta\nu = 700$ Hz where the average is over all orientations. The correlation frequency in hertz that corresponds to the collapse of this can be estimated²⁷ from $\nu_c = \delta\nu/2(2^{1/2})$ and the associated temperature can be obtained from the plot of π flip rate vs. inverse temperature in Figure 4. Furthermore, one can also justify adding frequency points corresponding to the temperatures of the maxima in dynamic mechanical⁴ and dielectric relaxation²⁶⁻²⁸ data as found in the literature. First, the previous work with the chloral polycarbonate indicated a good correlation between the dynamic mechanical loss peak at low temperature and the phenylene proton NMR data. Second, it has long been argued that an apparent coupling or cooperativity exists between phenylene group motion and motion involving the carbonate as evidenced by both dilute solution¹⁴ and solid-state experiments.⁶⁻⁷ A plot of the $\log \nu_c$ vs. T^{-1} containing the various experimental results is presented in Figure 6. A linear least-

squares analysis of these data allows for a determination of $E_A^* = 48$ kJ/mol from the slope and $\tau_{\infty}^* = 1.06 \times 10^{-16}$ s from the intercept.

The $T_{1\rho}$ and T_1 data can then be simulated by simply varying n and S , given the E_A^* and τ_{∞}^* from the relaxation map. The best fit as shown in Figure 2 was obtained with $n = 0.82$ and $S = 1.8 \times 10^{-2}$ mT². These values of the model parameters are physically reasonable. The activation energy of the fundamental process, E_A (obtained from the Ngai formalism in the absence of correlated state coupling), which has been identified as π flips of the phenylene rings, is 8.6 kJ/mol and can be compared to the dilute-solution value of 13 kJ/mol for phenylene rotation obtained in an earlier solution study.³¹ The solution activation energy should be slightly higher than E_A since even in a 10 wt % solution the surroundings will affect the fundamental process. The magnitude of n indicates that in the bulk glass the phenylene motion is strongly affected by the medium. The apparent activation energy in the glass is substantially higher, 48 kJ/mol. The value of S , the proton second moment, used in eq 14 should correspond to the motionally modulated component of the second moment. This motionally modulated dipole-dipole interaction corresponds to part of the intermolecular dipole-dipole contributions since the predominant motion causing modulation is phenylene ring motion about the C_1C_4 axis which does not reorient the largest intramolecular dipole-dipole interaction. The second moment is not given an explicit temperature dependence except through the spectral density as indicated by eq 14. A detailed proton line shape has not been carried out here but preliminary results indicate the second moment behavior parallels the earlier chloral polycarbonate study.¹⁰ The amount of motionally modulated second moment employed here is consistent with the experimental value of $(1.5 \pm 0.4) \times 10^{-2}$ mT² observed at the highest temperature of that study.

To further probe the success of this molecular modeling, the position and shape of the dynamic mechanical loss peak located at about -100 °C at 1 Hz, the γ peak as measured by Yee,⁴ was analyzed. The mechanical loss $G_{\gamma}(\omega)^{\text{loss}}$ is given by the equation

$$G_{\gamma}(\omega)^{\text{loss}} = \frac{\langle \sigma_{\gamma}(0)^2 \rangle}{k_B T} \int_0^{\infty} \sin(\omega t) \phi'(t) dt \quad (17)$$

where $\phi'(t)$ is the derivative of the correlation function. One sees in Figure 7 that much of the shape and temperature dependence is well simulated without further parameter adjustment of E_A^* , τ_{∞}^* , or n . The magnitude of the calculated loss peak is controlled by $\langle \sigma_{\gamma}(0) \rangle$, which is adjusted to match the data.

Discussion

Carbon-13 chemical shift anisotropy line shape analysis serves to definitively characterize the geometry of phenylene group motion as a combination of π flips and restricted rotation. The π flip rate is found to lie on a relaxation map containing proton T_1 and $T_{1\rho}$ minima, dielectric loss maxima, and dynamic mechanical loss maxima. This combination of such a broad sampling of frequency results in a more accurate time scale and activation energy analysis. A single exponential correlation function, as was used in the simple two-site jump model for the temperature dependence of the CSA line shapes, is inadequate for the simulation of the T_1 , $T_{1\rho}$, and dynamic mechanical loss data. It follows that the activation energy from a single correlation time analysis may be in serious error.

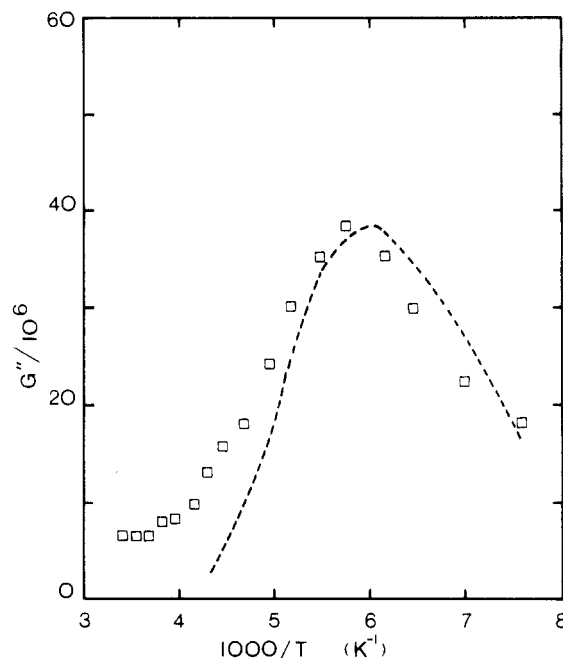


Figure 7. Dynamic mechanical spectrum. The dashed line is the simulation employing the Williams-Watts-Ngai fractional exponential with the parameters set from the relaxation map.

This phenomenological link in time between the various relaxation experiments can be quantitatively summarized in terms of a fractional exponential correlation function. This function reasonably approximates the shape and position of the T_1 and $T_{1\rho}$ minima vs. temperatures as well as the temperature position and breadth of the dynamic mechanical loss peak. Such a connection between the relaxation experiments argues for a common underlying dynamic process which produces NMR, dielectric, and mechanical relaxation.

There are, however, some questions raised by this conclusion. Jumps of the phenylene group between symmetric minima are unlikely to produce a large mechanical loss¹⁶ and certainly will not produce a dielectric loss. A recent proposal³² suggests that the common motion leading to the several relaxation effects is a correlated interchange³³ of carbonate group conformations. A cis-trans carbonate conformation is interchanged with a trans-trans carbonate conformation by rotations about backbone CO bonds. This motion reorients carbonate groups which could lead to dielectric and shear loss. The BPA unit between the two carbonates interchanging conformations is translated but not significantly reoriented. The π flips are tied to this correlated backbone motion by intramolecular and intermolecular interactions which places the π flips on a relaxation map in common with dielectric and dynamic mechanical loss peaks. While this proposed motion cannot be completely verified, it is however, consistent with the observed relaxation phenomena.

The fractional exponential used to summarize the relaxation phenomena is cast in the Ngai form and yields realistic values for the apparent activated energy E_A^* and the microscopic activation energy E_A . This aspect assumes the fractional exponential correlation function is homogeneous though this is not required to simulate the relaxation minima and loss maxima. Dilute-solution studies yield comparable values of E_A for both phenylene group rotation and correlated segmental motion which also appear to be linked in the dissolved polymer.¹⁴ Comparably low values for rotational barriers in BPA polycarbonate have been noted in theoretical calculations.³⁴⁻³⁵ These generally low barriers may be the key to the presence of

such extensive dynamic freedom in the glass as has been proposed by Tonelli³⁴ though only solid-state NMR line shape data have provided the basis to discriminate between various possible motions. Since virtually all intramolecular rotational barriers are low in polycarbonate and yet only certain reorientations are observed, intermolecular interactions must determine the nature of the motion in the glass. It is known that the BPA unit does not reorient except for π flips and restricted oscillation and this can be attributed to the difficulty of rotating such a large group in the glass. The proposed conformational interchange does not reorient the BPA unit though the smaller carbonate unit is reoriented. Again a conformational interchange is proposed so long-range chain end rotation or translation is not required. A carbon-13 CSA line shape study has also been carried out on the carbonate unit.³⁶ Little line shape change is noted here, which is difficult to reconcile with the presence of a large dielectric loss peak. However, the proposed conformational interchange involves a polycarbonate chain where most units are trans-trans and a smaller number of units are cis-trans. Thus, the carbonate unit would predominantly reflect the trans-trans CSA tensor and orientation. However, the conformational interchange leads to diffusion of the cis-trans conformation so all units can undergo reorientation though the time scale is complex.

The temperature dependence of the oscillation of the phenylene group about the C_1C_4 axis is also interesting. The rms amplitude is apparently linear vs. temperature to the one-half power, which is to be expected for a harmonic potential. However, the amplitude also ought to go to zero at a temperature of absolute zero for a harmonic potential. The simulation does not yield this result and the significance of the behavior shown in Figure 5 will be the subject of a subsequent paper.

Acknowledgment. This research was carried out with the financial support of the National Science Foundation Grant DMR-790677, of National Science Foundation Equipment Grant No. CHE77-09059, of National Science Foundation Grant No. DMR-8108679, and of U.S. Army Research Office Grant DAAG 29-82-G-0001.

Registry No. (Bisphenol A)-(carbonic acid) (copolymer), 25037-45-0; bisphenol A polycarbonate (SRU), 24936-68-3.

References and Notes

- (1) McCall, D. W. *Acc. Chem. Res.* 1971, 4, 223.
- (2) McBrierty, V. J.; Douglass, D. C. *Phys. Rep.* 1980, 63, 61.
- (3) Heijboer, J. J. *Polym. Sci., Part C* 1968, 16, 3755.
- (4) Yee, A. F.; Smith, S. A. *Macromolecules* 1981, 14, 54.
- (5) Matsuoka, S.; Ishida, Y. *J. Polym. Sci., Part C* 1966, 14, 247.
- (6) Massa, D. J.; Flick, J. R. *Polym. Prepr., Am. Chem. Soc., Div. Polym. Chem.* 1973, 14, 1249.
- (7) Massa, D. J.; Rusanowsky, R. P. *Polym. Prepr., Am. Chem. Soc., Div. Polym. Chem.* 1976, 17, 184.
- (8) Nielsen, L. E. "Mechanical Properties of Polymers and Composites"; Marcel Dekker: New York, 1974.
- (9) Schaefer, J.; Stejskal, E. O.; Buchdahl, R. *Macromolecules* 1977, 10, 384.
- (10) Inglefield, P. T.; Jones, A. A.; Lubianez, R. P.; O'Gara, J. F. *Macromolecules* 1981, 14, 288.
- (11) Jones, A. A.; O'Gara, J. F.; Inglefield, P. T.; Bendler, J. T.; Yee, A. F.; Ngai, K. L. *Macromolecules* 1983, 16, 685.
- (12) Inglefield, P. T.; Amici, R. M.; O'Gara, J. F.; Hung, C.-C.; Jones, A. A. *Macromolecules* 1983, 16, 1552.
- (13) Spiess, H. W. *Colloid Polym. Sci.* 1983, 261, 193.
- (14) Connolly, J. J.; Gordon, E.; Jones, A. A. *Macromolecules* 1984, 17, 722.
- (15) Schaefer, J.; Stejskal, E. O.; McKay, R. A.; Dixon, W. T. *Macromolecules* 1984, 17, 1479.
- (16) Garroway, A. N.; Ritchey, W. M.; Moniz, W. B. *Macromolecules* 1982, 15, 1051.
- (17) Ngai, K. L. *Comments Solid State Phys.* 1979, 9, 127.
- (18) Ngai, K. L.; White, C. T. *Phys. Rev. B* 1979, 20, 2475.
- (19) Ngai, K. L. *Phys. Rev. B* 1980, 22, 2066.
- (20) Williams, G.; Watts, D. C. *Trans. Faraday Soc.* 1970, 66, 80.
- (21) Schnell, H.; Krimm, A. *Angew. Chem., Int. Ed. Engl.* 1963, 2, 373.
- (22) Mehring, M. *NMR: Basic Princ. Prog.* 1976, 11.
- (23) Bloembergen, N.; Rowland, T. J. *Acta Metall.* 1955, 1, 731.
- (24) Slotfeldt-Ellingsen, D.; Resing, H. A. *J. Phys. Chem.* 1980, 84, 2204.
- (25) Wemmer, D. E. Ph.D. Thesis, University of California, Berkeley, CA, 1979.
- (26) Wemmer, D. E.; Ruben, D. J.; Pines, A. *J. Am. Chem. Soc.* 1981, 103, 28.
- (27) Sandstrom, J. "Dynamic NMR Spectroscopy"; Academic Press: New York, 1982.
- (28) Illers, K. H.; Breur, H. *Kolloid-Z.* 1961, 176, 110.
- (29) Krum, F.; Miller, F. H. *Kolloid-Z.* 1959, 1959, 164.
- (30) Michailov, G. P.; Eidelant, M. P. *Vysokomol. Soedin.* 1960, 2, 281.
- (31) Jones, A. A.; Bisceglia, M. *Macromolecules* 1979, 12, 136.
- (32) Jones, A. A., submitted for publication in *Macromolecules*.
- (33) Hall, C. K.; Helfand, E. *J. Chem. Phys.* 1982, 77, 3275.
- (34) Tonelli, A. E. *Macromolecules* 1972, 5, 558.
- (35) Bendler, J. T. *Ann. N. Y. Acad. Sci.* 1973, 6, 503. Bendler, J. T. *Ann. N. Y. Acad. Sci.* 1981, 371, 299.
- (36) Henrichs, P. M., submitted for publication in *Macromolecules*.